Acta Crystallographica Section F
Structural Biology and Crystallization Communications
ISSN 1744-3091

Crystallization of a truncated soluble human semicarbazide-sensitive amine oxidase

Emma Jakobsson,[a] Joakim Nilsson,[b] Ulla Källström,[b] Derek Ogg[b] and Gerard J. Kleywegt[a]*

[a]Department of Cell and Molecular Biology, Uppsala University, Biomedical Centre, Box 596, SE-751 24 Uppsala, Sweden, and [b]Research and Development, Biovitrum AB, Lindhagensgatan 133, SE-112 76 Stockholm, Sweden

Correspondence e-mail: gerard@xray.bmc.uu.se

Received 10 January 2005
Accepted 24 January 2005
Online 8 February 2005

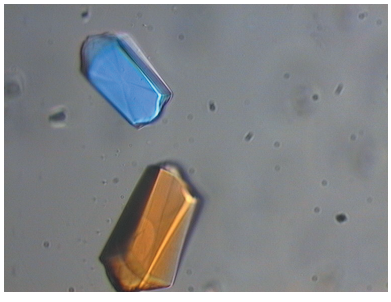

Human semicarbazide-sensitive amine oxidase (SSAO) is a homodimeric copper-containing monoamine oxidase that occurs in both a membrane-bound and a soluble form. SSAO is also known as vascular adhesion protein-1 (VAP-1). A truncated soluble form of human SSAO (comprising residues 29–763) was expressed in human embryonic kidney 293 cells and purified to homogeneity. Tetragonal crystals were obtained and a data set extending to 2.5 Å was collected. The crystals are merohedrally twinned and the estimation of the twinning fraction was complicated by pseudo-symmetry and the anisotropic character of the crystals. Using a recently developed method for twinning detection that is insensitive to phenomena such as anisotropy or pseudo-symmetry [Padilla & Yeates (2003), *Acta Cryst.* D**59**, 1124–1130], the twinning fraction was estimated to be 0.3. The structure was eventually solved by molecular replacement in space group $P4_3$.

1. Introduction

Semicarbazide-sensitive amine oxidase (SSAO; EC 1.4.3.6) belongs to a family of copper-containing amine oxidases (CuAOs) that carry out the oxidative deamination of primary amines to aldehydes, hydrogen peroxide and ammonia (Lyles, 1996; Jalkanen & Salmi, 2001; O'Sullivan *et al.*, 2004). Essential for the deamination reaction is the topa quinone (TPQ) cofactor derived from the post-translational modification of a tyrosine residue in the active site (Klinman, 2003). Benzylamine is a good non-physiological substrate for human SSAO and physiological substrates are believed to include methylamine and aminoacetone (Lyles, 1996; Yu *et al.*, 2003; O'Sullivan *et al.*, 2004). It has been speculated that human SSAO may also use free NH_2 groups on certain proteins and aminosugars as physiological substrates (Salmi *et al.*, 2001; Göktürk, Nilsson *et al.*, 2003; Koskinen *et al.*, 2004; Sibon *et al.*, 2004). Human SSAO is a glycosylated homodimeric type II membrane protein of approximately 170–180 kDa that is anchored by a single N-terminal transmembrane helix (Salmi & Jalkanen, 1996; Smith *et al.*, 1998), but it also exists in a soluble form circulating in the blood stream. Recent findings suggest that the soluble form of human SSAO is released by shedding of the membrane-anchored form (Göktürk, Nilsson *et al.*, 2003; Abella *et al.*, 2004; Stolen *et al.*, 2004).

Human SSAO may have several different physiological functions; for example, SSAO activity has been implicated in the regulation of adipocyte differentiation and glucose transport (Zorzano *et al.*, 2003), regulation of blood pressure (Göktürk, Nilsson *et al.*, 2003; Vidrio *et al.*, 2003) and elastic fibre organization (Langford *et al.*, 1999; Göktürk, Nilsson *et al.*, 2003; Sibon *et al.*, 2004). Furthermore, the amino-acid sequence of SSAO was found to be identical to that of vascular adhesion protein-1 (VAP-1), a protein with adhesive function involved in leukocyte transmigration through the endothelium into inflammation sites (Smith *et al.*, 1998; Salmi & Jalkanen, 2001). The enzymatic activity of SSAO/VAP-1 was recently found to be essential for the leukocyte extravasation process (Koskinen *et al.*, 2004). SSAO/VAP-1 is thus an example of a so-called 'moonlighting protein' (Jeffery, 1999; Tipton *et al.*, 2003), *i.e.* a protein with two or more distinct functions.

Elevated levels of soluble SSAO have been detected in several pathological conditions, particularly in diabetes mellitus, congestive heart failure and cirrhotic liver inflammation (Boomsma *et al.*, 2003).

It has been suggested that some of the complications associated with diabetes, such as retinopathy, nephropathy, neuropathy, atherosclerosis and cardiovascular complications, may be caused by toxic products of SSAO-catalysed reactions (Ekblom, 1998; Karádi *et al.*, 2002; Salmi *et al.*, 2002; Göktürk, Garpenstrand *et al.*, 2003).

The three-dimensional structure of CuAOs from *Escherichia coli* (PDB code 1oac; Parsons *et al.*, 1995), *Pisum sativum* (PDB code 1ksi; Kumar *et al.*, 1996), *Arthobacter globiformis* (PDB code 1av4; Wilce *et al.*, 1997) and *Hanensula polymorpha* (PDB code 1a2v; Li *et al.*, 1998) and of the lysyl oxidase from *Pichia pastoris* (PDB code 1n9e; Duff *et al.*, 2003) have been reported. They all share a similar fold and contain three domains called D2, D3 and D4. The highest degree of structural similarity between these CuAOs is observed for the central D4 β-sandwich domain, which contains the dimer interface. On the outside of the D4 domain there are two smaller α/β domains, D2 and D3. The first CuAO structure from *E. coli* was described as having the shape of a mushroom in which D2, D3 and D4 form the cap. In addition to these three domains, the *E. coli* protein contains a fourth domain, D1, which forms the stalk of the mushroom and D1–D1 interactions contribute to the dimer interface (Parsons *et al.*, 1995). The level of sequence identity between these CuAOs and human SSAO is 20–27%. The structure of bovine serum amine oxidase (BSAO) has recently been solved (PDB code 1tu5; Lunelli *et al.*, 2005). BSAO is the first mammalian CuAO structure to be reported and its sequence has 83% identity to human SSAO. However, the coordinates of this structure had not yet been released at the time of writing. A hexagonal crystal form of full-length human SSAO/VAP-1 (diffracting to 3.2 Å resolution) has been reported previously (Nymalm *et al.*, 2003), but to our knowledge this structure has not yet been published.

We have produced and crystallized an N-terminally truncated soluble form of human SSAO. The protein was truncated to exclude the putative transmembrane region and comprises residues 29–763 of the wild-type sequence. Tetragonal crystals were obtained with unit-cell parameters $a = b = 130.2$, $c = 221.5$ Å which diffracted to 2.5 Å at synchrotron sources. The structure could be solved in space group $P4_3$ by molecular-replacement techniques and its refinement is under way.

2. Material and methods

2.1. Construction of the SSAO mammalian expression vector

The construction of the expression vector and production of soluble SSAO will be described in detail elsewhere (Öhman *et al.*, 2005). Briefly, the region corresponding to residues 29–763 of human SSAO (AOC3; GenBank accession No. NM_003734) was isolated by PCR from plasmid pCIneo-hSSAO, which contains the complete coding sequence of human SSAO (Göktürk, Nilsson *et al.*, 2003). This fragment was introduced into a plasmid containing GST and a 3C protease cleavage site. The resulting GST-SSAO fragment was isolated and cloned into the mammalian expression vector pCI-neo (Promega) containing a cloned signal peptide for secretion of GST-SSAO. This vector, named pMB887, was used to develop stably transfected human embryonic kidney 293 (HEK293) cells expressing GST-SSAO.

2.2. Expression

Stably transfected HEK293 cells were thawed and seeded into T225 tissue-culture flasks containing pre-warmed Dulbecco's modified Eagle's growth medium (DMEM) supplemented with 862 mg l^{-1} L-alanyl-L-glutamine (GlutaMAX I, Gibco), 4.5 g l^{-1} D-glucose, 5% foetal bovine serum (FBS) and 1 mg ml^{-1} Geneticin and then grown at 310 K and 5% CO_2. The final sub-cultivation was performed in 20 collagen-coated roller bottles (RB; 850 cm^2, Corning). 4 d later, cells from all RBs were pooled and diluted into the supplemented growth medium described above. Using a Cellmate (The Automation Partnership, UK), the cells were distributed into 133 RBs (collagen-coated) to give a total volume of 220 ml growth medium in each RB. All RBs were grown in the presence of 5% CO_2 at 310 K and 0.2 rev min^{-1}. After 3 and 7 d, respectively, the medium was harvested and exchanged with supplemented growth medium containing a reduced amount of FBS (2%) and incubated as above. After an additional 3 d, the final harvest was performed, resulting in a total of 3 × 30 l harvested medium.

2.3. Purification

After filtration of the medium, each 30 l batch was concentrated (molecular-weight cutoff 30 kDa) to a final volume of 1 l. The GST-SSAO fusion protein was purified according to the manufacturer's recommendation on two serially mounted 5 ml GSTrap columns (Amersham Biosciences) equilibrated with phosphate-buffered saline (PBS). The protein material was loaded at 0.9 ml min^{-1} at room temperature. After washing the column with PBS, the fusion protein was eluted with 20 m*M* GSH, 0.1 *M* NaCl and 0.1 *M* Tris–HCl pH 8.2. The eluate was loaded onto a HiPrep Desalt 26/10 column (Amersham Biosciences) equilibrated with a cleavage buffer consisting of 150 m*M* NaCl, 1 m*M* EDTA and 50 m*M* Tris–HCl pH 7.5 at 298 K. The peak was collected and cleavage was started by adding dithiothreitol to a final concentration of 5 m*M* and 19 units of PreScission protease (Amersham Biosciences) per milligram of fusion protein. The cleavage mixture was incubated at 277 K for 60 h and then loaded onto a GSTrap column pre-equilibrated with cleavage buffer. Cleavage of the GST fusion protein leaves a native glycine, G29, at the N-terminus of the SSAO product. The flow-through was collected, concentrated (molecular-weight cutoff 30 kDa) and loaded onto a HiLoad 26/60 Superdex 200 prep-grade column (Amersham Biosciences) equilibrated with 150 m*M* NaCl and 50 m*M* Tris–HCl pH 7.5. Fractions containing SSAO were pooled, concentrated to 4 mg ml^{-1} in the above equilibration buffer and stored in aliquots at 193 K.

2.4. Crystallization, data collection and data processing

The initial crystallization conditions were obtained from trials carried out at the high-throughput crystallization facility of the Hauptman–Woodward Institute in Buffalo (Luft *et al.*, 2003). After

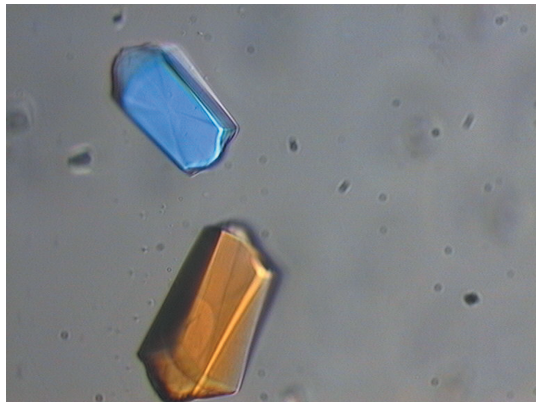

Figure 1
Tetragonal SSAO crystals. The crystals are colourless and their approximate dimensions are 0.3 × 0.15 × 0.1 mm.

optimization of these conditions, the best crystals were obtained by the hanging-drop vapour-diffusion method with 5 µl 4 mg ml^{-1} SSAO and 5 µl 0.1 *M* KBr, 0.1 *M* acetate pH 5.0, 38% PEG 1000 at 288 K. Crystals appeared after two to three weeks and grew to approximately 0.3 × 0.15 × 0.1 mm (Fig. 1). The first usable data set to 3 Å was collected at 100 K after flash-cooling the crystal in liquid nitrogen. More recently, a data set extending to 2.5 Å was collected in the same way. The data collections were performed at beamline ID14-1, ESRF, Grenoble, France using an ADSC Q4 CCD detector. Data processing, integration and scaling were performed with *MOSFLM* 6.2.4 (Leslie, 1992) and *SCALA* (Evans, 1997).

2.5. Structure solution

Use of the analysis method of Padilla & Yeates (2003), as implemented in *DATAMAN* (Kleywegt & Jones, 1996), revealed that the crystals were merohedrally twinned. The same test was used to estimate the twinning fraction. After detwinning the data with *DETWIN* (Taylor & Leslie, 1998), the structure was solved by molecular replacement with *AMoRe* (Navaza, 1994) using a polyalanine model of the dimer of domain D4 (residues 231–646) of *P. sativum* SSAO (PDB code 1ksi; Kumar *et al.*, 1996) as the search model. Data between 15 and 4.6 Å were used and the solution was obtained in space group $P4_3$.

3. Results and discussion

Crystals appeared under several conditions from the standard commercial screens. Some of these crystals diffracted to 3–4 Å, but no satisfactory cryoconditions could be found and the crystals were too radiation-sensitive to allow collection of more than a few degrees of data from each crystal at room temperature. Therefore, a protein sample was sent to the high-throughput crystallization facility at the Hauptman–Woodward Institute in Buffalo (Luft *et al.*, 2003) for further screening. A scan of 1536 sets of conditions yielded reproducible and diffracting crystals in three different conditions that were suitable for flash-freezing. Optimization of the initial conditions resulted in crystals that could be used for data collection.

The first usable data set was weak, extended to only 3 Å resolution and was anisotropic (data not shown). This data was indexed and merged in point group *P*422 and a molecular-replacement solution with one dimer in the asymmetric unit was obtained in space group $P4_32_12$. The maps looked promising and the search model was rebuilt in *O* (Jones *et al.*, 1991). However, after a few rounds of refinement with *CNS* (Brünger *et al.*, 1998) alternated with manual rebuilding in *O* the *R* factors were stuck around 0.45–0.50 and the maps did not improve. The density in domain D4 which was used to solve the structure looked acceptable, but it was very difficult to continue to build domains D2 and D3. At this point, the model mainly contained the correct residues in domain D4, but domains D2 and D3 still consisted of a polyalanine version of the corresponding domains in the search model 1ksi. To find out if the different domains could have shifted with respect to each other in human SSAO compared with pea seedling SSAO, rigid-body refinement was attempted with both *REFMAC*5 (Murshudov *et al.*, 1997) and *CNS*. Each monomer was split into four fragments, namely domains D2, D3 and D4 and a linker between domains D3 and D4. The first refinement step used data to 5 Å, the second run data to 4.5 Å and so on, increasing the resolution in steps of 0.5 Å until all data were included. At low resolution the rigid-body refinement yielded a small improvement of the *R* value, but as more data were included the *R* values actually increased. In search for an explanation for this unusual behaviour, we investigated whether the crystal could be twinned. Since twinning is not possible in space group $P4_32_12$, the crystal must in that case belong to the lower symmetry point group *P*4. The data set was submitted to the Merohedral Crystal Twinning Server (Yeates, 1997) and this showed that the crystal was indeed twinned, with an estimated twinning fraction of 0.4 according to this server, and that the true point group was thus *P*4. However, since the molecular-replacement solution in $P4_32_12$ was well packed and had reasonable *R* values, this also suggested that the crystal suffered from pseudo-symmetry.

Often, twinning can be detected in a cumulative intensity plot (Rees, 1980). However, the intensity distribution will deviate from that expected in the case of pseudo-symmetry and anisotropic data and the typical characteristics of twinned data can no longer be seen in the plot. Recently, Padilla & Yeates (2003) described a method for twinning detection that is insensitive to phenomena such as anisotropy and pseudo-symmetry. In this approach, nearby pairs of reflection intensities are compared. The method was implemented in *DATAMAN* and clearly revealed that the data were twinned (Fig. 2). However, even a data set that was detwinned with a twinning fraction of 0.4 did not look like an untwinned data set in the Padilla–Yeates plot. It is likely that the pseudo-symmetry (at low resolution) enhances the similarity of the reflections that are related owing to the twinning, which leads to an overestimation of the twinning fraction. Therefore, the data were detwinned using several different twinning fractions and the resulting detwinned data sets were in turn analysed with the Padilla–Yeates method. In this way, it was found that a twinning fraction of 0.25 resulted in a detwinned data set that behaved almost exactly like an untwinned one (Fig. 2). Clearly, if the utility of this method of estimating the twinning fraction were shown to be more general, it would be amenable to automation.

The molecular-replacement problem was subsequently solved from scratch using the reprocessed and detwinned data. Based on an

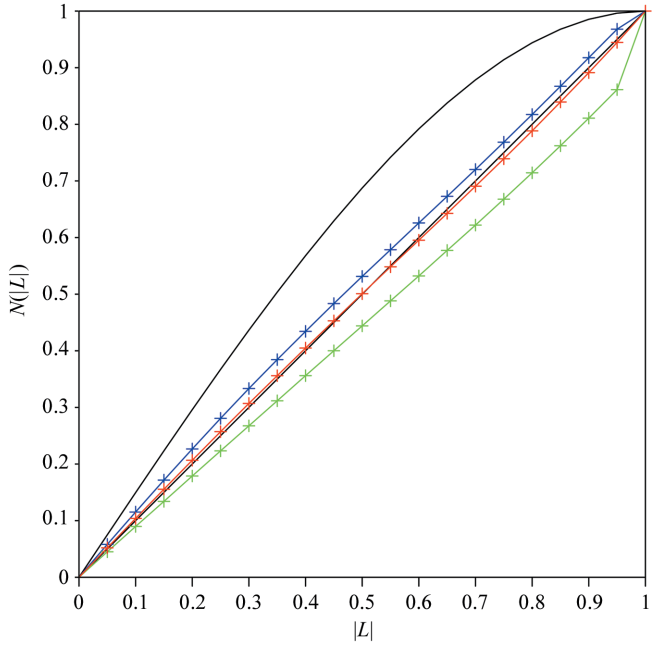

Figure 2
Local intensity statistics plot (Padilla & Yeates, 2003) calculated with *DATAMAN* (Kleywegt & Jones, 1996). The black diagonal shows the theoretical relationship for untwinned data and the curved black line that for perfectly twinned data. The curve for the twinned 3 Å SSAO data set is shown in blue. The curves for this data set after detwinning are shown in red (assumed twinning fraction 0.25) and green (assumed twinning fraction 0.4). Clearly, a twinning fraction of 0.25 has resulted in a data set that behaves almost the same as untwinned data.

analysis of the systematic absences along 00*l*, the translation function was only carried out in space groups $P4_1$ and $P4_3$. A polyalanine model of the dimer of domain D4 from *P. sativum* SSAO (PDB code 1ksi; Kumar *et al.*, 1996) was used as the search model. A clear solution with two dimers in the asymmetric unit was obtained in space group $P4_3$ and refinement of the structure was begun.

Subsequently, a data set to 2.5 Å was collected at beamline ID14-1, ESRF, Grenoble, France (Table 1, Fig. 3). This crystal suffered from the same problems as the earlier crystal (twinning, pseudo-symmetry, anisotropy) and the twinning fraction was estimated to be ∼0.3 by the method described above (data not shown). The anisotropic character of the data can be seen in Fig. 4. Refinement of the model was continued using this data set. At present, the model has an R value of 0.23 and $R_{\rm free}$ is 0.26. The results will be reported elsewhere.

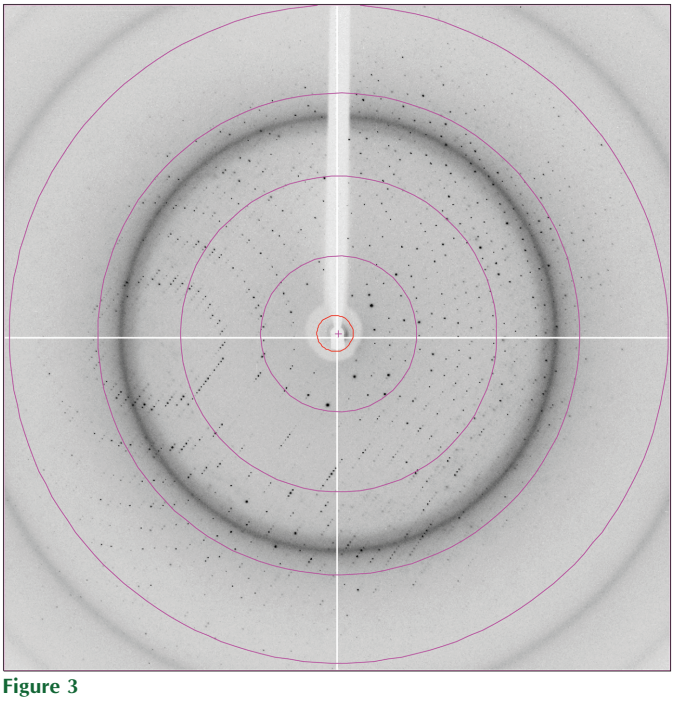

Figure 3
SSAO diffraction pattern. The resolution rings correspond to 10.1, 5.0, 3.3 and 2.5 Å. The figure was produced with *MOSFLM* (Leslie, 1992).

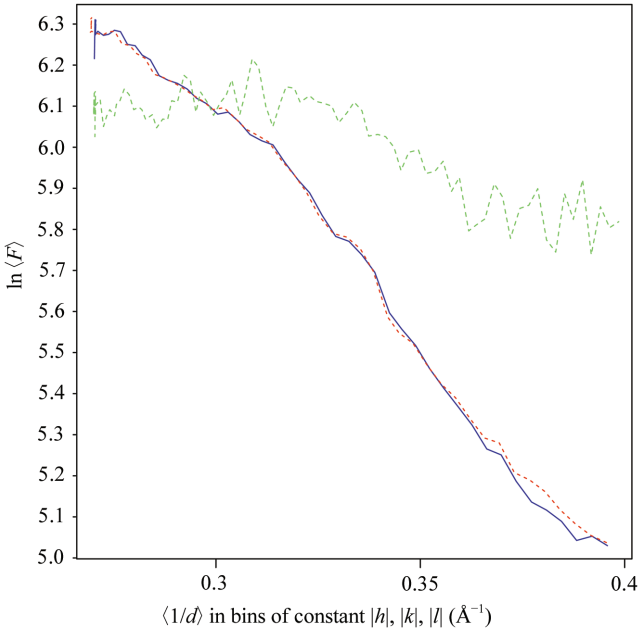

Figure 4
Anisotropy plot made using *DATAMAN* (Kleywegt & Jones, 1996). Sets of reflections with the same value of $|h|$, $|k|$ or $|l|$ are collected. For each set, the average value of the reciprocal resolution and the natural logarithm of the mean value of $F_{\rm obs}$ are calculated. The curve for bins of constant $|h|$ is plotted in blue, for constant $|k|$ in red and for constant $|l|$ in green.

Table 1
Data-collection, processing, scaling and merging statistics.

Values in parentheses are for the highest resolution shell.

Space group	$P4_3$
Unit-cell parameters (Å)	$a = b = 130.2$, $c = 221.5$
Resolution range (Å)	20.0–2.5 (2.64–2.5)
No. observations	656305 (70936)
No. unique reflections	126698 (18482)
Completeness (%)	99.8 (100.0)
$R_{\rm merge}$†	0.104 (0.438)
$\langle I/\sigma(I)\rangle$	13.8 (3.2)
Average redundancy	5.2 (3.8)
NCS (molecules per AU)	4 (2 homodimers)
$V_{\rm M}$ (Å^3 Da^{-1})	2.8
Solvent content (%)	55
Estimated twinning fraction	0.3
$\langle\|L\|\rangle$‡	0.468
$\langle L^2\rangle$‡	0.299

† $R_{\rm merge} = \sum_h \sum_i |I_{h,i} - \langle I_h\rangle| / \sum_h \sum_i |I_{h,i}|$, where the outer summation is over all unique reflections with multiple observations and the inner summation over all observations of each reflection. ‡ Padilla & Yeates (2003) statistics calculated using the observed data before detwinning. For untwinned data, $\langle|L|\rangle = 1/2$ and $\langle L^2\rangle = 1/3$; for perfectly merohedrally twinned data, $\langle|L|\rangle = 3/8$ and $\langle L^2\rangle = 1/5$.

Post hoc analysis of the molecular-replacement solution in space group $P4_3$ shows that the packing of the two homodimers is indeed very close to the packing in space group $P4_32_12$. The operator that relates the two dimers in space group $P4_3$ has a translational offset of 0.03 in fractional coordinates (corresponding to 6–7 Å) in the c direction and this breaks the symmetry in space group $P4_32_12$. In $P4_3$, the reflections with indices hkl and those with khl (which are equivalent in point group $P422$, but not necessarily in $P4$) can be merged with an $R_{\rm merge}(I)$ value of 0.079 for all data (0.044 for data between 130 and 4 Å, and 0.193 for data between 3 and 2.5 Å). Although these values are strikingly low, we are confident that the point-group symmetry is pseudo-$P422$ for a number of reasons. Firstly, the crystal was obviously twinned and thus cannot have $P422$ point-group symmetry. Secondly, if an intermediate model is used to calculate structure-factor intensities, then the $R_{\rm merge}$ values of the calculated data with indices hkl and khl are similar to (or less than) the values obtained with the observed data (namely, 0.047 for data between 130 and 4 Å and 0.113 for data between 3 and 2.5 Å). The situation with the SSAO crystal is therefore the opposite of that recently described by Rudiño-Piñera *et al.* (2004), whose tetragonal crystals of the ^{2}F1^{3}F1 module pair of human fibronectin were eventually shown to be untwinned and to belong to point group $P422$.

We wish to thank Dr Martin Norin (Biovitrum) who initiated the collaboration between the two laboratories. EJ and GJK wish to thank Nancy Fehrman of the high-throughput crystallization laboratory at the Hauptman–Woodward Institute in Buffalo (NY) for help with crystal-growth screening and the staff at the European Synchrotron Radiation Facility (ESRF) for help with data collection. EJ is supported through a grant from the Swedish Structural Biology Network (SBNet) to GJK. GJK is a Royal Swedish Academy of Sciences (KVA) Research Fellow, supported through a grant from the Knut and Alice Wallenberg Foundation.

References

Abella, A., Garcia-Vicente, S., Viguerie, N., Ros-Baro, A., Camps, M., Palacin, M., Zorzano, A. & Marti, L. (2004). *Diabetologia*, **47**, 429–438.

Boomsma, F., Bhaggoe, U. M., van der Houwen, A. M. B. & van den Meiracker, A. H. (2003). *Biochim. Biophys. Acta*, **1647**, 48–54.

Brünger, A. T., Adams, P. D., Clore, G. M., DeLano, W. L., Gros, P., Grosse-Kunstleve, R. W., Jiang, J.-S., Kuszewski, J., Nilges, M., Pannu, N. S., Read, R. J., Rice, L. M., Simonson, T. & Warren, G. L. (1998). *Acta Cryst.* D**54**, 905–921.

Duff, A. P., Cohen, A. E., Ellis, P. J., Kuchar, J. A., Langley, D. B., Shepard, E. M., Dooley, D. M., Freeman, H. C. & Guss, J. M. (2003). *Biochemistry*, **42**, 15148–15157.

Ekblom, J. (1998). *Pharmacol. Res.* **37**, 87–92.

Evans, P. R. (1997). *Jnt CCP4/ESF–EACBM Newsl. Protein Crystallogr.* **33**, 22–24.

Göktürk, C., Garpenstrand, H., Nilsson, J., Nordquist, J., Oreland, L. & Forsberg-Nilsson, K. (2003). *Biochim. Biophys. Acta*, **1647**, 88–91.

Göktürk, C., Nilsson, J., Nordquist, J., Kristensson, M., Svensson, K., Söderberg, C., Israelson, M., Garpenstrand, H., Sjöquist, M., Oreland, L. & Forsberg-Nilsson, K. (2003). *Am. J. Pathol.* **163**, 1921–1928.

Jalkanen, S. & Salmi, M. (2001). *EMBO J.* **20**, 3893–3901.

Jeffery, C. J. (1999). *Trends Biochem. Sci.* **24**, 8–11.

Jones, T. A., Zou, J. Y., Cowan, S. W. & Kjeldgaard, M. (1991). *Acta Cryst.* A**47**, 110–119.

Karádi, I., Mészáros, Z., Csányi, A., Szombathy, T., Hosszúfalusi, N., Romics, L. & Magyar, K. (2002). *Clin. Chim. Acta*, **323**, 139–146.

Kleywegt, G. J. & Jones, T. A. (1996). *Acta Cryst.* D**52**, 826–828.

Klinman, J. P. (2003). *Biochim. Biophys. Acta*, **1647**, 131–137.

Koskinen, K., Vainio, P. J., Smith, D. J., Pihlavisto, M., Ylä-Herttuala, S., Jalkanen, S. & Salmi, M. (2004). *Blood*, **103**, 3388–3395.

Kumar, V., Dooley, D. M., Freeman, H. C., Guss, J. M., Harvey, I., McGuirl, M. A., Wilce, M. C. & Zubak, V. M. (1996). *Structure*, **4**, 943–955.

Langford, S. D., Trent, M. B., Balakumaran, A. & Boor, P. J. (1999). *Toxicol. Appl. Pharmacol.* **155**, 237–244.

Leslie, A. G. W. (1992). *Jnt CCP4/ESF-–EACBM Newsl. Protein Crystallogr.* **26**.

Li, R., Klinman, J. P. & Mathews, F. S. (1998). *Structure*, **6**, 293–307.

Luft, J. R., Collins, R. J., Fehrman, N. A., Lauricella, A. M., Veatch, C. K. & DeTitta, G. T. (2003). *J. Struct. Biol.* **142**, 170–179.

Lunelli, M., Di Paolo, M. L., Biadene, M., Calderone, V., Battistutta, R., Scarpa, M., Rigo, A. & Zanotti, G. (2005). In the press.

Lyles, G. A. (1996). *Int. J. Biochem. Cell Biol.* **28**, 259–274.

Murshudov, G. N., Vagin, A. A. & Dodson, E. J. (1997). *Acta Cryst.* D**53**, 240–255.

Navaza, J. (1994). *Acta Cryst.* A**50**, 157–163.

Nymalm, Y., Kidron, H., Söderholm, A., Viitanen, L., Kaukonen, K., Pihlavisto, M., Smith, D., Veromaa, T., Airenne, T. T., Johnson, M. S. & Salminen, T. A. (2003). *Acta Cryst.* D**59**, 1288–1290.

Öhman, J., Jakobsson, E., Källström, U., Elmblad, A., Ansari, A., Kalderén, C., Robertson, E., Danielsson, E., Gustavsson, A.-L., Varadi, A., Ekblom, J., Holmgren, E., Doverskog, M., Abrahamsén, L. & Nilsson, J. (2005). In preparation.

O'Sullivan, J., Unzeta, M., Healy, J., O'Sullivan, M. I., Davey, G. & Tipton, K. F. (2004). *Neurotoxicology*, **25**, 303–315.

Padilla, J. E. & Yeates, T. O. (2003). *Acta Cryst.* D**59**, 1124–1130.

Parsons, M. R., Convery, M. A., Wilmot, C. M., Yadav, K. D., Blakeley, V., Corner, A. S., Phillips, S. E., McPherson, M. J. & Knowles, P. F. (1995). *Structure*, **3**, 1171–1184.

Rees, D. (1980). *Acta Cryst.* A**36**, 578–581.

Rudiño-Piñera, E., Schwarz-Linek, U., Potts, J. R. & Garman, E. F. (2004). *Acta Cryst.* D**60**, 1341–1345.

Salmi, M. & Jalkanen, S. (1996). *J. Exp. Med.* **183**, 569–579.

Salmi, M. & Jalkanen, S. (2001). *Trends Immunol.* **22**, 211–216.

Salmi, M., Stolen, C., Jousilahti, P., Yegutkin, G. G., Tapanainen, P., Janatuinen, T., Knip, M., Jalkanen, S. & Salomaa, V. (2002). *Am. J. Pathol.* **161**, 2255–2262.

Salmi, M., Yegutkin, G. G., Lehvonen, R., Koskinen, K., Salminen, T. & Jalkanen, S. (2001). *Immunity*, **14**, 265–276.

Sibon, I., Larrieu, D., El Hadri, K., Mercier, N., Feve, B., Lacolley, P., Labat, C., Daret, D., Bonnet, J. & Lamaziere, J. M. (2004). *J. Histochem. Cytochem.* **52**, 1459–1466.

Smith, D. J., Salmi, M., Bono, P., Hellman, J., Leu, T. & Jalkanen, S. (1998). *J. Exp. Med.* **188**, 17–27.

Stolen, C. M., Yegutkin, G. G., Kurkijärvi, R., Bono, P., Alitalo, K. & Jalkanen, S. (2004). *Circ. Res.* **95**, 50–57.

Taylor, H. O. & Leslie, A. G. W. (1998). *Jnt CCP4/ESF–EACBM Newsl. Protein Crystallogr.* **35**, 9.

Tipton, K. F., O'Sullivan, M. I., Davey, G. P. & O'Sullivan, J. (2003). *Biochem. Soc. Trans.* **31**, 711–715.

Vidrio, H., Medina, M., Gonzalez-Romo, P., Lorenzana-Jimenez, M., Diaz-Arista, P. & Baeza, A. (2003). *J. Pharmacol. Exp. Ther.* **307**, 497–504.

Wilce, M. C., Dooley, D. M,. Freeman, H. C., Guss, J. M., Matsunami, H., McIntire, W. S., Ruggiero, C. E., Tanizawa, K. & Yamaguchi, H. (1997). *Biochemistry*, **36**, 16116–16133.

Yeates, T. O. (1997). *Methods Enzymol.* **276**, 344–358.

Yu, P. H., Wright, S., Fan, E. H., Lun, Z.-R. & Gubisne-Haberle, D. (2003). *Biochim. Biophys. Acta*, **1647**, 193–199.

Zorzano, A., Abella, A., Marti, L., Carpéné, C., Palacín, M. & Testar, X. (2003). *Biochem. Biophys. Acta*, **1647**, 3–9.